A Novel Calibration Algorithm for a Special Class of Multiport Vector Network Analyzers

A Novel Calibration Algorithm for a Special Class of Multiport Vector Network Analyzers

Andrea Ferrero, *Senior Member, IEEE*, Valeria Teppati, *Member, IEEE*, Marco Garelli, *Student Member, IEEE*, and Alessandra Neri

***Abstract*—A new error model for a special class of multiport vector network analyzers (VNAs) is presented in this paper. This model can be applied to multiport network analyzers with noncomplete reflectometers, i.e., when the measurement of the incident waves at each port is not always available. The method used to compute the error coefficients proposed here is based on a compact and easy formulation. This method is an extension of the already existing general theory for complete reflectometer multiport network analyzers. Furthermore, the new error model generalizes the theory for three-sampler two-port VNAs. The proposed model has been tested against the complete reflectometer one and exhibits the same accuracy level.**

***Index Terms*—Calibration models, multiport network analyzer, multiport network analyzer calibration, vectorial error correction, vector network analyzer (VNA), VNA calibration.**

I. Introduction

With THE recent outstanding increase in the speed and complexity of digital systems and circuits, multiport characterization at microwaves and millimeter waves is undergoing an impressive increase in demand and importance. From the initial (somewhat limited) multiport monolithic microwave integrated circuit (MMIC) scope, the application of multiport techniques is shifting towards computer technologies: digital integrated circuits (ICs), microprocessors, high-speed printed circuit board (PCB) interconnections, and signal integrity [1]. The main requirements of these new applications are easily summarized as follows:

- large number of ports;
- reduced test costs;
- accurate and fast measurements;
- custom calibrations, to minimize the standard sequence.

In the early 1980s, the first multiport characterizations were performed with multiple (*round robin*) measurements with two-port vector network analyzers (VNAs) and matched loads on the unused ports [2]–[5]. These techniques are still in use today. Although it is possible to take into account the nonidealities of the matched terminations [6], [7], the procedure is cumbersome and the accuracy is affected by the multiple connections required.

Another approach is the use of multiport network analyzers [8], [9]. There are many possible ways of realizing multiport VNAs [10], ranging from the simpler architectures, based on a two-port network analyzer and complex switch matrices, to the more complex ones, with one source and a complete reflectometer for each port, like the one shown in Fig. 1(a). The latter offers the best calibration flexibility, but it is also the most expensive.[1]

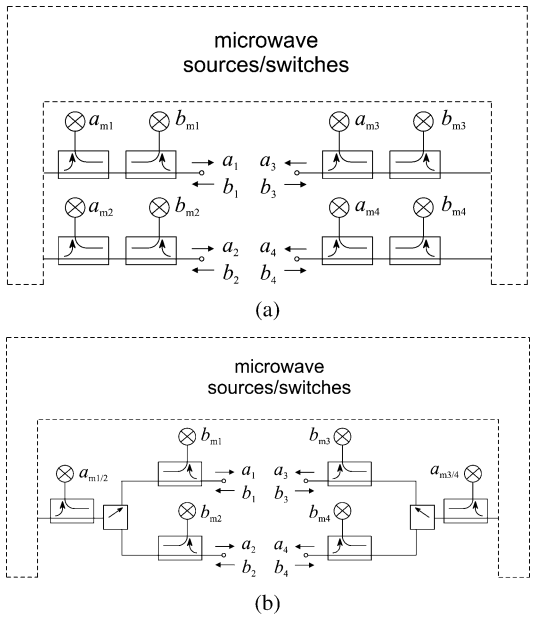

Fig. 1. (a) Complete reflectometer multiport architecture. (b) Example of the reduced architecture.

A good compromise, in terms of cost and complexity, is the *noncomplete reflectometer* architecture, shown in Fig. 1(b). This solution has been successfully applied to the currently available high-end commercial multiport VNAs [11].

This architecture has two reference channels and one measurement sampler for each port. Not all the incident waves are measured at the same time, which is an advantage in terms of speed, but a drawback in terms of flexibility. There are no general approaches for the calibration of these systems, i.e., they are specified for a fixed number of ports (typically 4 or 8), and use redundant standard sequences [10], [12].

In this paper, we will present an extension of the complete reflectometer multiport error-model [13] to the noncomplete reflectometer architecture, which allows flexible and customizable standard sequences.

Manuscript received June 7, 2007; revised November 8, 2007.

The authors are with the Dipartimento di Elettronica, Politecnico di Torino, 10100 Turin, Italy (e-mail: ferrero@polito.it; valeria.teppati@polito.it; marco.garelli@polito.it; alessandra.neri@polito.it).

Digital Object Identifier 10.1109/TMTT.2008.916952

[1]Rohde&Schwarz, Munich, Germany, Vector Network Analyzer R&S ZVA, 2006.

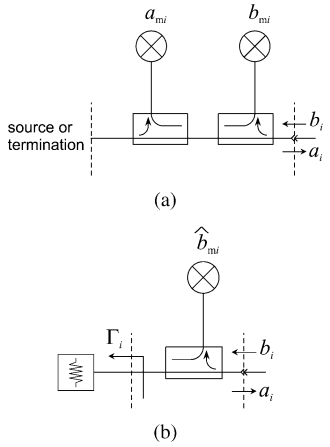

Fig. 2. (a) State A and (b) B configurations.

The basic model equations are defined in Section II, while Section III gives the new formulas for error coefficient computation and deembedding and also shows how the ten-term model [14] for two-port VNAs is a particular case of the proposed multiport model.

A technique that can be used to reduce the number of standard connections to the minimum is shown in Section IV. A practical example described here uses the minimum number of thrus and only one termination at one port. Other examples are presented in Section IV. Some conclusions are drawn in Section V.

II. Problem Definition

The error model proposed here is an extension of the complete multiport nonleaky model [13], to the case when complete reflectometers are not available for all the ports at the same time [see Fig. 1(b)].

Due to the presence of switches in the measurement paths, we make the assumption that each port has the following two different states:

- **State A** (the traditional one): complete reflectometer [see Fig. 2(a)];
- **State B**: partial reflectometer, i.e., only the reflected wave can be measured [see Fig. 2(b)].

In the following, these types of multiport systems are called *two-state multiport systems*, and their error model is called a *two-state model*.

The following equations [8]:

$$\begin{aligned} a_i &= l_i b_{\mathrm{m}i} - h_i a_{\mathrm{m}i} \\ b_i &= k_i b_{\mathrm{m}i} - m_i a_{\mathrm{m}i} \end{aligned} \tag{1}$$

represent state A, while

$$\begin{aligned} a_i &= g_i \hat{b}_{\mathrm{m}i} \\ b_i &= f_i \hat{b}_{\mathrm{m}i} \end{aligned} \tag{2}$$

are introduced here for state B.

Our assumption is that Γ_i, i.e., port i reflectometer termination in state B, is always the same for each port j source excitation with $i \neq j$ [see Fig. 2(b)], thus, the error model terms f_i and g_i do not vary with the reference switch positions.

In order to have corrected multiport scattering data, the coefficients l_i, m_i, h_i, k_i, f_i, and g_i first need to be computed for each port and then a deembedding procedure must be applied.

III. Two-State Model—General Formulation

Let (1) and (2) be in matrix form for an n port system

$$\begin{aligned} \boldsymbol{a} &= \boldsymbol{L}\boldsymbol{b}_{\mathrm{m}} - \boldsymbol{H}\boldsymbol{a}_{\mathrm{m}} \\ \boldsymbol{b} &= \boldsymbol{K}\boldsymbol{b}_{\mathrm{m}} - \boldsymbol{M}\boldsymbol{a}_{\mathrm{m}} \\ \boldsymbol{a} &= \boldsymbol{G}\hat{\boldsymbol{b}}_{\mathrm{m}} \\ \boldsymbol{b} &= \boldsymbol{F}\hat{\boldsymbol{b}}_{\mathrm{m}} \end{aligned} \tag{3}$$

where

$$\boldsymbol{a} = \begin{pmatrix} a_1 \\ a_2 \\ \vdots \\ a_n \end{pmatrix} \quad \boldsymbol{b} = \begin{pmatrix} b_1 \\ b_2 \\ \vdots \\ b_n \end{pmatrix} \tag{4}$$

$$\boldsymbol{a}_{\mathrm{m}} = \begin{pmatrix} a_{\mathrm{m}1} \\ a_{\mathrm{m}2} \\ \vdots \\ a_{\mathrm{m}n} \end{pmatrix} \quad \boldsymbol{b}_{\mathrm{m}} = \begin{pmatrix} b_{\mathrm{m}1} \\ b_{\mathrm{m}2} \\ \vdots \\ b_{\mathrm{m}n} \end{pmatrix} \tag{5}$$

$$\hat{\boldsymbol{b}}_{\mathrm{m}} = \begin{pmatrix} \hat{b}_{\mathrm{m}1} \\ \hat{b}_{\mathrm{m}2} \\ \vdots \\ \hat{b}_{\mathrm{m}n} \end{pmatrix} \tag{6}$$

and

$$\boldsymbol{X} = \begin{bmatrix} x_1 & 0 & \cdots & 0 \\ 0 & x_2 & \cdots & 0 \\ \vdots & \vdots & \ddots & \vdots \\ 0 & 0 & \cdots & x_n \end{bmatrix} \tag{7}$$

where $\boldsymbol{X}$ is the generic error coefficient matrix, i.e., $\boldsymbol{X} = \boldsymbol{M}, \boldsymbol{H}, \boldsymbol{K}, \boldsymbol{L}, \boldsymbol{F}$, and $\boldsymbol{G}$, with $x = m, h, k, l, f$, and g. As already mentioned, leakage is neglected, thus these matrices are all diagonal.

An equation such as (3) can be written for each of the n source signal positions. These n equations can be stacked together to form a unique matrix equation

$$\begin{aligned} \boldsymbol{A} &= \boldsymbol{L}\boldsymbol{B}_{\mathrm{m}} - \boldsymbol{H}\boldsymbol{A}_{\mathrm{m}} \\ \boldsymbol{B} &= \boldsymbol{K}\boldsymbol{B}_{\mathrm{m}} - \boldsymbol{M}\boldsymbol{A}_{\mathrm{m}} \end{aligned} \tag{8}$$

where $\boldsymbol{A}$, $\boldsymbol{B}$, $\boldsymbol{A}_{\mathrm{m}}$, and $\boldsymbol{B}_{\mathrm{m}}$ are square $n \times n$ matrices defined as

$$\begin{aligned} \boldsymbol{A} &= [\boldsymbol{a}_1\, \boldsymbol{a}_2 \ldots \boldsymbol{a}_n] \\ \boldsymbol{B} &= [\boldsymbol{b}_1\, \boldsymbol{b}_2 \ldots \boldsymbol{b}_n] \\ \boldsymbol{A}_{\mathrm{m}} &= [\boldsymbol{a}_{\mathrm{m}1}\, \boldsymbol{a}_{\mathrm{m}2} \ldots \boldsymbol{a}_{\mathrm{m}n}] \\ \boldsymbol{B}_{\mathrm{m}} &= [\boldsymbol{b}_{\mathrm{m}1}\, \boldsymbol{b}_{\mathrm{m}2} \ldots \boldsymbol{b}_{\mathrm{m}n}] \end{aligned} \tag{9}$$

where $\boldsymbol{a}_i$ and $\boldsymbol{b}_i$ are the reference plane wave vectors of (4) and $\boldsymbol{a}_{\mathrm{m}i}$ and $\boldsymbol{b}_{\mathrm{m}i}$ are the measured wave vectors of (5) for the ith source signal position.

Since the device-under-test (DUT) imposes the well-known equation

$$\boldsymbol{b} = \boldsymbol{S}\boldsymbol{a} \tag{10}$$

using (9), we obtain

$$\boldsymbol{B} = \boldsymbol{S}\boldsymbol{A}. \tag{11}$$

By substituting (8) in (11), we find the equation for the error coefficient computation

$$\boldsymbol{S}\boldsymbol{L}\boldsymbol{B}_{\mathrm{m}} - \boldsymbol{S}\boldsymbol{H}\boldsymbol{A}_{\mathrm{m}} - \boldsymbol{K}\boldsymbol{B}_{\mathrm{m}} + \boldsymbol{M}\boldsymbol{A}_{\mathrm{m}} = \boldsymbol{0} \tag{12}$$

or for deembedding

$$\boldsymbol{S} = (\boldsymbol{K}\boldsymbol{B}_{\mathrm{m}} - \boldsymbol{M}\boldsymbol{A}_{\mathrm{m}})(\boldsymbol{L}\boldsymbol{B}_{\mathrm{m}} - \boldsymbol{H}\boldsymbol{A}_{\mathrm{m}})^{-1}. \tag{13}$$

Equation (12) can be expanded as

$$\sum_{p=1}^{n} S_{ip} l_p b_{\mathrm{m}pj} - \sum_{p=1}^{n} S_{ip} h_p a_{\mathrm{m}pj} - k_i b_{\mathrm{m}ij} + m_i a_{\mathrm{m}ij} = 0, \qquad i = 1, \ldots, n; \quad j = 1, \ldots, n. \tag{14}$$

Equations (12)–(14) are written in terms of measured waves rather than measured S-parameters, as in [9].

In other words, no switch correction technique has been applied here to obtain the measured scattering matrix. The calibration equations are written directly in terms of the measured quantities.

If $\boldsymbol{B}_{\mathrm{m}}$ and $\boldsymbol{A}_{\mathrm{m}}$ were completely known from the measurements, this would solve the calibration problem.

Instead, the two-state architecture does not allow all the incident and reflected waves to be measured simultaneously. We deal with the case where the quantities $a_{\mathrm{m}ij}$ and $b_{\mathrm{m}ij}$ with $i \neq j$ are not directly accessible, i.e., port i is always in state B when the source is at port j and only the $\hat{b}_{\mathrm{m}ij}$ measurements are known.

In this case, matrices $\boldsymbol{A}_{\mathrm{m}}$ and $\boldsymbol{B}_{\mathrm{m}}$ can be seen as the sum of diagonal matrices $\tilde{\boldsymbol{A}}_{\mathrm{m}}$ and $\tilde{\boldsymbol{B}}_{\mathrm{m}}$, which contain actual measurements, and $\boldsymbol{A}'_{\mathrm{m}}$ and $\boldsymbol{B}'_{\mathrm{m}}$, which have null diagonals and contain all the other not directly measured waves

$$\begin{aligned} \boldsymbol{A}_{\mathrm{m}} &= \tilde{\boldsymbol{A}}_{\mathrm{m}} + \boldsymbol{A}'_{\mathrm{m}} \\ \boldsymbol{B}_{\mathrm{m}} &= \tilde{\boldsymbol{B}}_{\mathrm{m}} + \boldsymbol{B}'_{\mathrm{m}} \end{aligned} \tag{15}$$

where

$$\tilde{\boldsymbol{B}}_{\mathrm{m}} \equiv \begin{bmatrix} b_{\mathrm{m}11} & 0 & \cdots & 0 \\ 0 & b_{\mathrm{m}22} & \cdots & 0 \\ \vdots & \vdots & \ddots & \vdots \\ 0 & 0 & \cdots & b_{\mathrm{m}nn} \end{bmatrix} \tag{16}$$

$$\tilde{\boldsymbol{A}}_{\mathrm{m}} \equiv \begin{bmatrix} a_{\mathrm{m}11} & 0 & \cdots & 0 \\ 0 & a_{\mathrm{m}22} & \cdots & 0 \\ \vdots & \vdots & \ddots & \vdots \\ 0 & 0 & \cdots & a_{\mathrm{m}nn} \end{bmatrix}. \tag{17}$$

An expression is now found for $\boldsymbol{A}_{\mathrm{m}}$ and $\boldsymbol{B}_{\mathrm{m}}$, as a function of $\tilde{\boldsymbol{B}}_{\mathrm{m}}$ and $\hat{\boldsymbol{B}}_{\mathrm{m}}$, which is defined as

$$\hat{\boldsymbol{B}}_{\mathrm{m}} \equiv \begin{bmatrix} 0 & \hat{b}_{\mathrm{m}12} & \hat{b}_{\mathrm{m}13} & \cdots & \hat{b}_{\mathrm{m}1n} \\ \hat{b}_{\mathrm{m}21} & 0 & \hat{b}_{\mathrm{m}23} & \cdots & \hat{b}_{\mathrm{m}2n} \\ \hat{b}_{\mathrm{m}31} & \hat{b}_{\mathrm{m}32} & 0 & \cdots & \hat{b}_{\mathrm{m}3n} \\ \vdots & \vdots & \ddots & \ddots & \vdots \\ \hat{b}_{\mathrm{m}n1} & \hat{b}_{\mathrm{m}n2} & \cdots & \hat{b}_{\mathrm{m}nn-1} & 0 \end{bmatrix}. \tag{18}$$

Models A and B must represent the same physical condition, i.e., the waves at the DUT reference planes computed with the two models must be the same. In other words, for the same source excitation j, the waves a_{ij} and b_{ij} must be independent of the error model. Therefore, we can obtain the unmeasured $a_{\mathrm{m}ij}$ and $b_{\mathrm{m}ij}$ from (1) and (2) by imposing the condition

$$\begin{pmatrix} b_{\mathrm{m}ij} \\ a_{\mathrm{m}ij} \end{pmatrix} = \begin{bmatrix} l_i & -h_i \\ k_i & -m_i \end{bmatrix}^{-1} \begin{pmatrix} g_i \\ f_i \end{pmatrix} \hat{b}_{\mathrm{m}ij} = \begin{pmatrix} \alpha_i \\ \beta_i \end{pmatrix} \hat{b}_{\mathrm{m}ij} \tag{19}$$

where

$$\begin{aligned} \alpha_i &= \frac{h_i f_i - m_i g_i}{k_i h_i - l_i m_i} \\ \beta_i &= \frac{l_i f_i - k_i g_i}{k_i h_i - l_i m_i}. \end{aligned} \tag{20}$$

In this case (the source is at port j), we can write

$$\boldsymbol{a}_{\mathrm{m}j} = \begin{pmatrix} \beta_1 \hat{b}_{\mathrm{m}1j} \\ \beta_2 \hat{b}_{\mathrm{m}2j} \\ \vdots \\ a_{\mathrm{m}jj} \\ \vdots \\ \beta_n \hat{b}_{\mathrm{m}nj} \end{pmatrix} \quad \boldsymbol{b}_{\mathrm{m}j} = \begin{pmatrix} \alpha_1 \hat{b}_{\mathrm{m}1j} \\ \alpha_2 \hat{b}_{\mathrm{m}2j} \\ \vdots \\ b_{\mathrm{m}jj} \\ \vdots \\ \alpha_n \hat{b}_{\mathrm{m}nj} \end{pmatrix}. \tag{21}$$

By defining

$$\alpha \equiv \begin{bmatrix} \alpha_1 & 0 & \cdots & 0 \\ 0 & \alpha_2 & \cdots & 0 \\ \vdots & \vdots & \ddots & \vdots \\ 0 & 0 & \cdots & \alpha_n \end{bmatrix} \tag{22}$$

$$\beta \equiv \begin{bmatrix} \beta_1 & 0 & \cdots & 0 \\ 0 & \beta_2 & \cdots & 0 \\ \vdots & \vdots & \ddots & \vdots \\ 0 & 0 & \cdots & \beta_n \end{bmatrix} \tag{23}$$

we find the expressions for $\boldsymbol{A}_{\mathrm{m}}$ and $\boldsymbol{B}_{\mathrm{m}}$ as follows:

$$\begin{aligned} \boldsymbol{A}_{\mathrm{m}} &= \tilde{\boldsymbol{A}}_{\mathrm{m}} + \beta \hat{\boldsymbol{B}}_{\mathrm{m}} \\ \boldsymbol{B}_{\mathrm{m}} &= \tilde{\boldsymbol{B}}_{\mathrm{m}} + \alpha \hat{\boldsymbol{B}}_{\mathrm{m}}. \end{aligned} \tag{24}$$

Since it is easy to demonstrate from (20) that

$$\begin{aligned} \boldsymbol{G} &\equiv \boldsymbol{L}\alpha - \boldsymbol{H}\beta \\ \boldsymbol{F} &\equiv \boldsymbol{K}\alpha - \boldsymbol{M}\beta \end{aligned} \tag{25}$$

by substituting (24) in (12), we obtain

$$-\boldsymbol{S}\boldsymbol{G}\hat{\boldsymbol{B}}_{\mathrm{m}}+\boldsymbol{F}\hat{\boldsymbol{B}}_{\mathrm{m}}-\boldsymbol{S}\boldsymbol{L}\tilde{\boldsymbol{B}}_{\mathrm{m}}+\boldsymbol{K}\tilde{\boldsymbol{B}}_{\mathrm{m}}+\boldsymbol{S}\boldsymbol{H}\tilde{\boldsymbol{A}}_{\mathrm{m}}-\boldsymbol{M}\tilde{\boldsymbol{A}}_{\mathrm{m}}=\boldsymbol{0}. \tag{26}$$

This generalized system can be used to compute the error coefficients (i.e., matrices $\boldsymbol{H}$, $\boldsymbol{K}$, $\boldsymbol{L}$, $\boldsymbol{M}$, $\boldsymbol{F}$, and $\boldsymbol{G}$) from the standard measurements and definitions.

For this purpose, it is useful to write the n^2 equations as follows:

$$\begin{aligned}-\sum_{p=1}^{n}(1-\delta_{pj})S_{ip}g_p\hat{b}_{\mathrm{m}pj}+(1-\delta_{ij})f_i\hat{b}_{\mathrm{m}ij}-S_{ij}l_jb_{\mathrm{m}jj}\\ +\delta_{ij}k_ib_{\mathrm{m}ij}+S_{ij}h_ja_{\mathrm{m}jj}\\ -\delta_{ij}m_ia_{\mathrm{m}ij}=0,\qquad i=1,\ldots,n;\quad j=1,\ldots,n\end{aligned} \tag{27}$$

where δ_{ij} is the Kronecker delta. In order to avoid the trivial zero solution, the homogeneous system is normalized to one of the unknown coefficients, thus, the total number of unknown error coefficients will be $6n-1$, instead of $4n-1$, as in the complete reflectometer model [8].

The exception to this rule is the two-port case, where the system splits into two homogeneous systems and (27) become

$$\begin{cases}-S_{12}g_2\hat{b}_{\mathrm{m}21}+(k_1-S_{11}l_1)b_{\mathrm{m}11}+\ldots\\ \qquad\qquad\ldots+(S_{11}h_1-m_1)a_{\mathrm{m}11}=0\\ (f_2-S_{22}g_2)\hat{b}_{\mathrm{m}21}-S_{21}l_1b_{\mathrm{m}11}+S_{21}h_1a_{\mathrm{m}11}=0\end{cases} \tag{28}$$

and

$$\begin{cases}-S_{21}g_1\hat{b}_{\mathrm{m}12}+(k_2-S_{22}l_2)b_{\mathrm{m}22}+\ldots\\ \qquad\qquad\ldots+(S_{22}h_2-m_2)a_{\mathrm{m}22}=0\\ (f_1-S_{11}g_1)\hat{b}_{\mathrm{m}12}-S_{12}l_2b_{\mathrm{m}22}+S_{12}h_2a_{\mathrm{m}22}=0.\end{cases} \tag{29}$$

Since (28) can be normalized to k_1 and (29) to k_2, the total number of coefficients in only ten, and these are easily mapped, as shown in the Appendix, onto the error-box terms of the traditional forward/reverse model for the two-port VNA described by Marks in [14].

Finally, from (24), the deembedding equation is

$$\boldsymbol{S}=(\boldsymbol{K}\tilde{\boldsymbol{B}}_{\mathrm{m}}-\boldsymbol{M}\tilde{\boldsymbol{A}}_{\mathrm{m}}+\boldsymbol{F}\hat{\boldsymbol{B}}_{\mathrm{m}})(\boldsymbol{L}\tilde{\boldsymbol{B}}_{\mathrm{m}}-\boldsymbol{H}\tilde{\boldsymbol{A}}_{\mathrm{m}}+\boldsymbol{G}\hat{\boldsymbol{B}}_{\mathrm{m}})^{-1}. \tag{30}$$

IV. Application Examples

Some experiments have been performed to validate the proposed methodology using actual multiport coaxial systems. One of the setups that have been used is based on a 6-GHz Anritsu MS4623 coupled with a four-port expansion box (MMS0518B) from PAF, Turin, Italy [15], whose reflectometer architecture is shown in Fig. 3. This allows a comparison of the complete reflectometer model and the proposed two-state model to be made, simply by neglecting the nonmeasurable quantities when necessary.

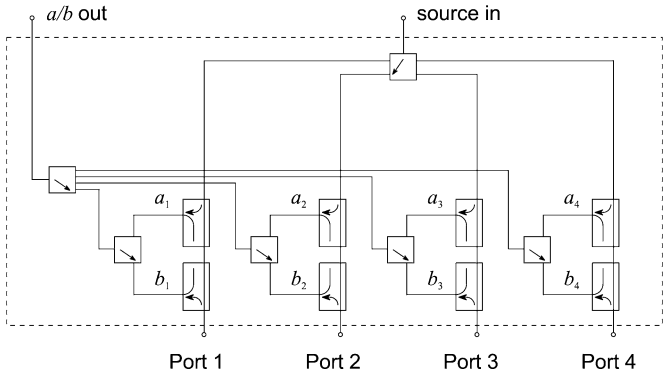

Fig. 3. Simplified MMS0518B block scheme.

As usual, the calibration can be performed by measuring one-, two-, or n-port standards. In particular, if we consider a two-reference architecture, like the one in Fig. 1(b), a two-port standard can be measured as follows:

- with both ports in state A at the same time (state AA);
- with one port in state A and the other in state B (state AB) and vice versa (state BA).

It should be noted that (14) and (27) can be stacked together in a single system, where (14) is used if the standard is measured in state AA, while (27) is used if the standard is measured in state AB–BA.

In other words, the presence of two reference channels in the architecture will allow some standard measurements to be in state AA, as well as in state AB–BA, thus adding useful equations to the system and simplifying the standard sequence.

As a first example, let us consider a three-port thru loop calibration [9] consisting of the following standards:

- 50-Ω load at port 1;
- thru 1–2;
- thru 2–3;
- thru 1–3;

which is the simplest multiport VNA calibration available, and has proven to be very accurate [16]. In order to have zero-length thrus, we chose to use APC7 connectors.

As shown in [9], this calibration is consistent with the complete reflectometer calibration model if each two-port measurement can be taken in the AA state. The number of independent equations provided by the two-port standards is, in fact, $4n-2$. With the addition of the one-port standard, the number of independent equation becomes $4n-1$, which is equal to the number of the unknowns for a complete reflectometer system using the complete reflectometer calibration model.

It has been verified, by numerical simulations, that this calibration is also consistent for the new two-state model if two "sides" of the loop can be measured in both state AA and state AB–BA, while one side is measured only in state AB–BA, as sketched in Fig. 4. The overall error model has a larger number of unknowns ($6n-1$), but eight equations, rather than four, are obtained from the thru measurements in the AA and AB–BA states.

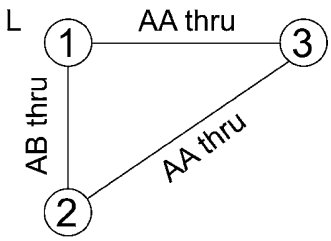

Fig. 4. Thru loop calibration example for a two-state system.

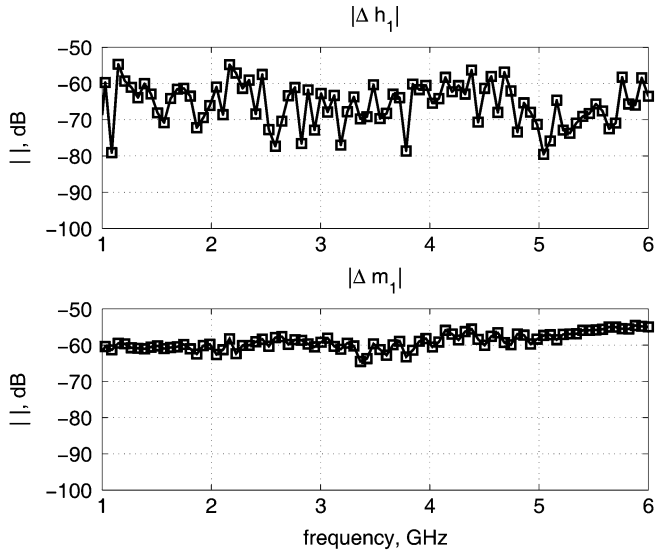

Fig. 5. Error coefficient comparison. Δh_1 (and Δm_1) are the differences between coefficients h_1 (and m_1) computed with the two different calibrations, i.e.: 1) thru loop, with only AA measurements (complete reflectometer model) and 2) thru loop, with an AB side (two-state model).

The following two calibrations were then compared:

- thru loop, with only AA measurements (complete reflectometer model);
- thru loop, with an AB side (two-state model).

First the error coefficients l_i, m_i, h_i, and k_i $(i = 1, 2, 3)$ were compared. They are practically the same for the two calibrations. The absolute values of Δh_1 (and Δm_1) in decibels (e.g., $20 \cdot \log_{10} |\Delta h_1|$) are shown in Fig. 5 as an example.

The results of the two calibrations on the same raw data were then compared and no noticeable differences were found. An example is shown in Fig. 6 for a coaxial line. Other comparisons, for a four-port example, are reported here. We compare two calibrations, both based on the following standard sequence:

- short-open-load port 1;
- thru 1–3;
- thru 2–3;
- thru 1–4;

i.e., Quick SOLT-type [17] calibrations extended to the multiport. As a benchmark, a complete reflectometer model calibration is performed with all the standard measurements in the AA state. It is compared to a partial reflectometer model calibration, with all thrus measured in both state AA and state AB–BA. The measurements of a four-port 180°, 2–18 GHz, hybrid are then performed. With the complete reflectometer model, measurements are performed in state A for each one of the four ports, i.e., incident waves are always measured. With the partial reflectometer model, during the measurements, the incident waves at each port are measured only when the source is switched to that port. This makes the partial reflectometer measurement much faster than the complete reflectometer one. The results of this comparison are reported in Fig. 7, and show that the two calibration models are not discernible.

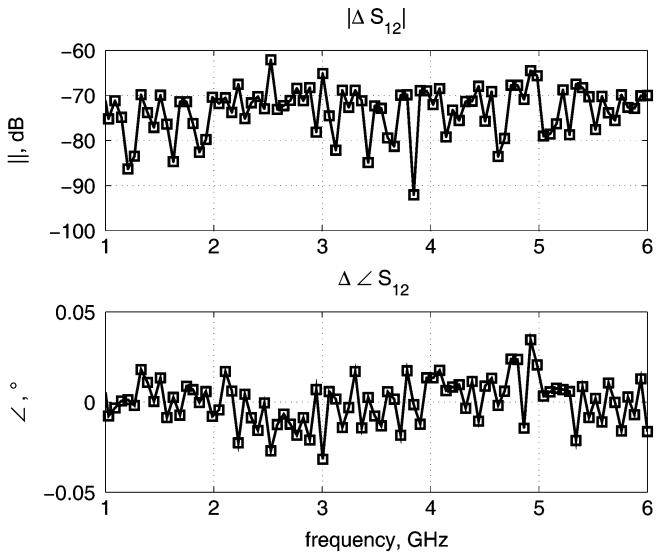

Fig. 6. Measurement of transmission coefficient of a coaxial line. ΔS_{12} is the difference between the transmission parameter S'_{12} computed with algorithm 1) and S''_{12} computed with algorithm 2). $\Delta \angle S_{12}$ is the difference between the transmission parameter phases, computed with the two different algorithms.

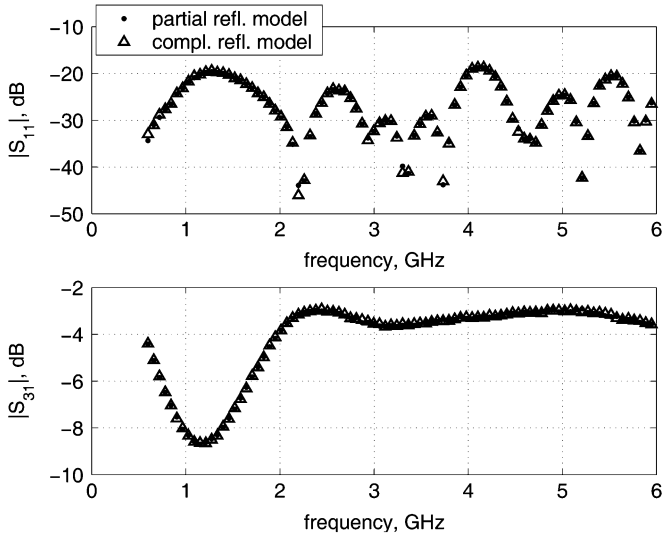

Fig. 7. Measurements of a commercial 2–18-GHz 180° hybrid coupler with an all state A, complete reflectometer model calibration, and a partial reflectometer calibration.

These and other measurement results are encouraging and suggest that the novel two-state model gives faster results with the same accuracy level as the complete reflectometer one.

V. Conclusion

A new and simplified error model for noncomplete reflectometer multiport VNAs has been presented. A generalized, compact formulation for error coefficient extraction has been found, validated through experiments, and performed in a coaxial environment, and very good results have been found. The proposed model is expected to fulfill the new requirements

of speed, high number of ports, and accuracy required for high-speed computer technologies and signal integrity tests.

APPENDIX

Here we will show the transformation of the traditional ten-term forward/reverse model for two-port VNAs, described by Marks in [14], into the model proposed in this study.

For the ten-term model, the following equations represent the forward case:

$$a_1 = a_{m1} + E_{SF} b_1 \tag{A1}$$
$$b_{m1} = E_{DF} a_{m1} + E_{RF} b_1 \tag{A2}$$
$$\hat{b}_{m2} = E_{TF} b_2 \tag{A3}$$
$$a_2 = E_{LF} b_2 \tag{A4}$$

while for the reverse case, we have

$$a_2 = a_{m2} + E_{SR} b_2 \tag{A5}$$
$$b_{m2} = E_{DR} a_{m2} + E_{RR} b_2 \tag{A6}$$
$$\hat{b}_{m1} = E_{TR} b_1 \tag{A7}$$
$$a_1 = E_{LR} b_1. \tag{A8}$$

We can rearrange these equations as follows:

$$a_1 = \frac{E_{SF}}{E_{RF}} b_{m1} - \frac{\Delta_F}{E_{RF}} a_{m1} \tag{A9}$$
$$b_1 = \frac{1}{E_{RF}} b_{m1} - \frac{E_{DF}}{E_{RF}} a_{m1} \tag{A10}$$
$$a_2 = \frac{E_{LF}}{E_{TF}} \hat{b}_{m2} \tag{A11}$$
$$b_2 = \frac{1}{E_{TF}} \hat{b}_{m2} \tag{A12}$$

where $\Delta_F = E_{SF} E_{DF} - E_{RF}$, and

$$a_2 = \frac{E_{SR}}{E_{RR}} b_{m2} - \frac{\Delta_R}{E_{RR}} a_{m2} \tag{A13}$$
$$b_2 = \frac{1}{E_{RR}} b_{m2} - \frac{E_{DR}}{E_{RR}} a_{m2} \tag{A14}$$
$$a_1 = \frac{E_{LR}}{E_{TR}} \hat{b}_{m1} \tag{A15}$$
$$b_1 = \frac{1}{E_{TR}} \hat{b}_{m1} \tag{A16}$$

where $\Delta_R = E_{SR} E_{DR} - E_{RR}$.

By comparing these equations with (1) and (2), for $i = 1, 2$, we find the relationships between the two models

$$h_1 = \frac{\Delta_F}{E_{RF}} \quad l_1 = \frac{E_{SF}}{E_{RF}} \tag{A17}$$
$$k_1 = \frac{1}{E_{RF}} \quad m_1 = \frac{E_{DF}}{E_{RF}} \tag{A18}$$
$$h_2 = \frac{\Delta_R}{E_{RR}} \quad l_2 = \frac{E_{SR}}{E_{RR}} \tag{A19}$$
$$k_2 = \frac{1}{E_{RR}} \quad m_2 = \frac{E_{DR}}{E_{RR}} \tag{A20}$$
$$f_1 = \frac{1}{E_{TR}} \quad g_1 = \frac{E_{LR}}{E_{TR}} \tag{A21}$$
$$f_2 = \frac{1}{E_{TF}} \quad g_2 = \frac{E_{LF}}{E_{TF}}. \tag{A22}$$

REFERENCES

[1] S. Sercu and L. Martens, "Characterizing n-port packages and interconnections with a 2-port network analyzer," in *IEEE 6th Elect. Performance Electron. Packag. Top. Meeting*, Oct. 1997, pp. 163–166.

[2] J.-C. Tippet and R.-A. Speciale, "A rigorous technique for measuring the scattering matrix of a multiport device with a 2-port network analyzer," *IEEE Trans. Microw. Theory Tech.*, vol. MTT-30, no. 5, pp. 661–666, May 1982.

[3] U. Lott, W. Baumberger, and U. Gisiger, "Three-port RF characterization of foundry dual gate FETs using two-port test structures with on-chip loading resistors," in *Proc. IEEE Int. Microelectron. Test Structures Conf.*, Mar. 1995, pp. 167–180.

[4] C. S. Hartmann and R. T. Hartmann, "Software for multi-port RF network analysis with a large number of frequency samples and application to 5-port SAW device measurement," in *Proc. Ultrason. Symp.*, Dec. 1990, vol. 1, pp. 117–122.

[5] H.-C. Lu and T.-H. Chu, "Multiport scattering matrix measurement using a reduced-port network analyzer," *IEEE Trans. Microw. Theory Tech.*, vol. 51, no. 5, pp. 1525–1533, May 2003.

[6] J.-C. Rautio, "Techniques for correcting scattering parameter data of an imperfectly terminated multiport when measured with a two-port network analyzer," *IEEE Trans. Microw. Theory Tech.*, vol. MTT-31, no. 5, pp. 407–412, May 1983.

[7] M. Davidovits, "Reconstruction of the S-matrix for a 3-port using measurements at only two ports," *IEEE Trans. Microw. Theory Tech.*, vol. 5, no. 10, pp. 349–350, Oct. 1995.

[8] A. Ferrero, U. Pisani, and K. Kerwin, "A new implementation of a multiport automatic network analyzer," *IEEE Trans. Microw. Theory Tech.*, vol. 40, no. 11, pp. 2078–2085, Nov. 1992.

[9] A. Ferrero, F. Sampietro, and U. Pisani, "Multiport vector network analyzer calibration: A general formulation," *IEEE Trans. Microw. Theory Tech.*, vol. 42, no. 12, pp. 2455–2461, Dec. 1994.

[10] J. Martens, D. Judge, and J. Bigelow, "Multiport vector network analyzer measurements," *IEEE Micro.*, vol. 6, no. 4, pp. 72–81, Dec. 2005.

[11] Agilent Technol., Santa Clara, CA, "N4421BH67 S-parameter test set," 2006.

[12] H. Heuermann, "GSOLT: The calibration procedure for all multi-port vector network analyzers," in *IEEE MTT-S Int. Microw. Symp. Dig.*, Jun. 2003, vol. 3, pp. 1815–1818.

[13] A. Ferrero and F. Sanpietro, "A simplified algorithm for leaky network analyzer calibration," *IEEE Microw. Guided Wave Lett.*, vol. 5, no. 4, pp. 119–121, Apr. 1995.

[14] R. Marks, "Formulations of the basic vector network analyzer error model including switch-terms," in *50th Fall ARFTG Conf. Dig.*, Portland, OR, Dec. 1997, vol. 32, pp. 115–126.

[15] *"MMS Multiport Measurement System Manual,"* PAF, Turin, Italy, 2004. [Online]. Available: www.pafmicro.com

[16] F. Sanpietro, A. Ferrero, U. Pisani, and L. Brunetti, "Accuracy of a multiport network analyzer," *IEEE Trans. Instrum. Meas.*, vol. 44, no. 2, pp. 304–307, Apr. 1995.

[17] A. Ferrero and U. Pisani, "QSOLT: A new fast calibration algorithm for two port S parameter measurements," in *38th Winter ARFTG Conf. Dig.*, San Diego, CA, Dec. 1991, vol. 20, pp. 15–24.

Andrea Ferrero (S'85–M'87–SM'06) was born in Novara, Italy, on November 7, 1962. He received the Electronic Engineering degree and Ph.D. degree in electronics from the Politecnico di Torino, Turin, Italy, in 1987 and 1992, respectively.

In 1998, he joined the Aeritalia Company as a Microwave Consultant. He was with the Microwave Technology Division, Hewlett-Packard Company, Santa Rosa, CA, as a Summer Student in 1991. In 1995, he was with the Department of Electrical Engineering, Ecole Polytechnique de Montréal, Montréal, QC, Canada, as a Guest Researcher. In 1998 and 2006, he became an Associate and Full Professor in electronic measurements with the Dipartimento di Elettronica, Politecnico di Torino, respectively. His main research activities are in the area of microwave measurement techniques, calibration, and modeling.

Dr. Ferrero was the recipient of the 2006 ARFTG Technology Award for the development and implementation of VNA calibration algorithms and nonlinear measurement techniques.

Valeria Teppati (S'01–M'03) was born in Turin, Italy, on October 20, 1974. She received the Electronic Engineering degree and Ph.D. degree in electronic instrumentation from the Politecnico di Torino, Turin, Italy, in 1999 and 2003, respectively.

Since 2003, she has been with the Dipartimento di Elettronica, Politecnico di Torino, as a Research and Teaching Assistant. Since 2005, she has been an Assistant Professor with the Politecnico di Torino. Her research interests and activities include microwave device design, linear and nonlinear measurement design, multiports, calibration, and uncertainty.

Marco Garelli (S'04) was born in Cuneo, Italy, in 1981. He received the Electronic Engineering degree from the Politecnico di Torino, Turin, Italy, in 2005, and is currently working toward the Ph.D. degree in metrology at the Politecnico di Torino.

His main research interests are RF and microwave measurement techniques, including noise measurements.

Alessandra Neri was born in Ceva, Italy, in 1982. She received the Electronic Engineering degree from the Politecnico di Torino, Turin, Italy, in 2006, and is currently working toward the Ph.D. degree in metrology at the Politecnico di Torino.